Increasing the Corrosion Protection of AISI 1008 Carbon Steel by Surface Treatment with Unmodified and Benzotriazole Modified Sol-Gel Films

4250:497

The Williams Honors College

Shane Kelliher

4/23/2021

Table of Contents

Abstract

The corrosion performance of sol-gel coated AISI 1008 carbon steel was investigated in 3.5 wt% NaCl solutions of pH 7, 9, and 12 using electrochemical measurements. Sol-gel coatings were synthesized using two organopolysiloxane precursors: methacryloxypropyltrimethoxysilane (MAPTMS) and tetraethylorthosilicate (TEOS). A corrosion inhibitor, benzotriazole (BTA) was added to the sol-gel mixture and tested as a second, modified sol-gel coating. Sol-gel films adhered evenly to metal samples and were characterized by FTIR spectroscopy. Electrochemical Impedance Spectroscopy (EIS) showed an increase in polarization resistance from blank to sol-gel coated samples (600-18,800,000 ohms). Cyclic polarization (CPP) curves showed positive hysteresis loops for blank and unmodified sol-gel coated samples which increased at high pH following the backward potential scan, suggesting destruction to the passive film and pitting corrosion. The hysteresis loops for BTA modified sol-gel coated carbon steel followed an opposite trend with very little damage following polarization. CPP also confirmed a lower corrosion current density and more positive corrosion potential for sol-gel films (avg: 0.0019 $\mu A/cm^2$ and 94.7 mV/SCE for BTA modified sol-gel film) vs. blank samples (avg: 94.7 $\mu A/cm^2$ and -540 mV/SCE). While unmodified sol-gel films slightly increased the corrosion protection of AISI 1008 carbon steel, BTA modified sol-gel coated carbon steel exhibited the highest protection by far, obtaining an average corrosion rate of 0.000022 mm/yr, nearly three orders of magnitude lower than blank samples.

Executive Summary

Problem Statement

Infrastructure failure due to the corrosion of carbon steel is a very significant problem that costs the United States roughly $8.3 billion each year. AISI 1008 carbon steel is an alloy frequently used in reinforced concrete, which holds up thousands of bridges across the country. This study aimed to develop and test a technique for surface treatment of AISI 1008 carbon steel with sol-gel films in efforts to increase longevity of reinforced concrete. Sol-gel films were synthesized using two organopolysiloxane precursors: methacryloxypropyltrimethoxysilane (MAPTMS) and tetraethylorthosilicate (TEOS). The addition of a corrosion inhibitor, benzotriazole (BTA) was tested alongside an unmodified sol-gel coating. FTIR spectroscopy and electrochemical corrosion testing (OCP, EIS, CPP) were used to characterize the presence of coatings and determine the corrosion behavior of sol-gel coated carbon steel in 3.5 wt% NaCl solutions of varying pH (7, 9, 12).

Results

FTIR spectroscopy confirmed the homogeneous adherence of unmodified sol-gel and BTA modified sol-gel films on AISI 1008 carbon steel. Further, electrochemical testing provided Nyquist plots **(Figures 10-12)** and cyclic polarization curves **(Figures 13-15)** which identified polarization resistance, corrosion current density, and corrosion potential for coated and uncoated samples in all solutions. It was verified from electrochemical data that corrosion performance increased from pH 7 solution to pH 9 and 12 solutions. Cyclic polarization curves showed a higher damage following polarization as pH increased for blank and unmodified sol-gel coated carbon steel; however, the opposite trend was observed for BTA modified sol-gel coated samples. Most

notably, BTA modified sol-gel coated carbon steel had a significantly lower tendency of corrosion (nearly three magnitudes) in every solution when compared to unmodified sol-gel coated and blank carbon steel. A graphical corrosion rate comparison between carbon steel samples in all pH solutions can be viewed in Figure 18.

Conclusions

It was concluded that the presence of the unmodified sol-gel film slightly decreased the tendency of corrosion for AISI 1008 carbon steel. However, the addition of BTA to the sol-gel matrix immensely improved corrosion performance by nearly three orders of magnitude. The addition of BTA led nitrogen atoms on the inhibitor to bind with the surface of the metal, greatly slowing the charge transfer in the system. It was also concluded that damage to the unmodified sol-gel film occurred following polarization, evident by large, positive hysteresis loops following the backward potential scan. This showed that pitting corrosion was very likely for blank and unmodified sol-gel coated carbon steel, especially in higher pH solutions where passivity was achieved.

Implications

The broader implications of this work are immense. First, an incredible amount of laboratory experience was gained as hours each week were spent preparing/coating samples, making solutions, running electrochemical tests, etc. Second, the research involved with this project led to enhanced knowledge on the subject of coatings and inhibitors, along with the ability to use corrosion modelling software which will be very useful for the future. Lastly, and most important, this study led to the discovery of an effective coating technique for AISI 1008 carbon steel, which can potentially be used in industry for reinforced concrete, allowing increased longevity and lower risk of failure for many infrastructures.

Recommendations

Further testing is recommended to confirm the results presented in this study. Different molar ratios of MAPTMS and TEOS for sol-gel preparation should be experimented with, along with different amounts of BTA added to the sol-gel matrix. A higher range of solution pH along with different concentration of NaCl could also be tested. Lastly, SEM/XRD (Scanning Electron Microscope/X-Ray Diffraction) could be used prior to electrochemical testing for characterization of the sol-gel films, and post electrochemical testing to clearly identify specimen damage, pitting, corrosion products, etc.

Introduction

AISI 1008 carbon steel is used in a wide range of industry applications including machinery framing, pipelines, and reinforced concrete. The corrosion of carbon steel is a detrimental problem that puts numerous high scale infrastructures at risk of failure. Specific to concrete applications, the repair of reinforced concrete costs $200 per square meter of exposed surface. In the United States, the cost of concrete corrosion in highway bridges alone totals $8.3 billion each year, including maintenance, replacement, and capital costs [1]. The severity of the problem is increased as casualties are possible when infrastructure fails during commercial use. For instance, in May 2000 in Concord North Carolina, over 100 people were injured when steel strands corroded in a pre-stressed concrete pedestrian bridge leading the structure to collapse onto the highway below [1]. Corrosion of reinforced concrete is often a difficult issue to spot as the surface of the steel can rust and weaken while left unseen, embedded in the concrete.

The ambiguity of concrete corrosion suggests a need for enhanced protection of steel reinforcement. In this study, the effects of surface treatment with unmodified sol-gel and benzotriazole modified sol-gel films are investigated in pertinence to the corrosion behavior of AISI 1008 carbon steel. Previous work by Gelling and Galván suggests that coating AA2024-T3 alloy with sol-gel films increases corrosion protection, thus prolonging the lifespan and performance of the alloy in industry [2]. Similar sol-gel films were utilized in this study, with the primary objective of determining the degree of protection achieved for coated AISI 1008 carbon steel samples. An unmodified sol-gel containing methacryloxypropyltrimethoxysilane (MAPTMS) and tetraethylorthosilicate (TEOS), along with a benzotriazole modified sol-gel containing benzotriazole (BTA), MAPTMS, and TEOS were used as coatings. Experimental methods include FTIR spectroscopy, open circuit potential (OCP), potentiostatic electrochemical

impedance spectroscopy (EIS), and cyclic polarization (CPP), where corrosion rates can be determined and compared for samples in solutions of 3.5 wt% NaCl and varying pH.

Background

The basic corrosion mechanism of reinforced carbon steel in concrete includes the anodic dissolution of iron and the reduction of oxygen shown in equations (1) and (2). Furthermore, the Fe^{2+} from the anodic reaction can react with the product of the oxygen reduction reaction ($2OH^-$) to form a corrosion product ($Fe(OH)_2$) on the surface of the steel, shown in equation (3). In high pH solutions, a protective oxide film can form according to equation (4).

$$Fe \rightarrow Fe^{2+} + 2e^- \quad (1)$$

$$\frac{1}{2}O_2 + H_2O + 2e^- \rightarrow 2OH^- \quad (2)$$

$$Fe^{2+} + 2OH^- \rightarrow Fe(OH)_2 \quad (3)$$

$$2Fe(OH)_2 + \frac{1}{2}O_2 \rightarrow Fe_2O_3 + 2H_2O \quad (4)$$

When chlorides are present in solution, reinforced carbon steel is susceptible to pitting corrosion. Chlorides can penetrate the concrete through the pore network and micro cracks, accelerating the corrosion reaction and concrete deterioration. The passive film of the steel is broken when enough chlorides are present in the pore solution [3]. When chlorides are absorbed into the film, they can react with oxidized iron to form a soluble intermediate $(FeCl_4)^{2-}$ shown in equation (5). Further, this intermediate reacts with moisture to form $Fe(OH)_2$, $2H^+$, and $4Cl^-$ described by equation (6).

$$Fe^{2+} + 4Cl^- \rightarrow (FeCl_4)^{2-} + 2e^- \quad (5)$$

$$(FeCl_4)^{2-} + 2H_2O \rightarrow Fe(OH)_2 + 2H^+ + 4Cl^- \quad (6)$$

As these reactions occur, the pH is lowered, and the chloride concentration is increased. As chlorides are continuously released, the pitting process becomes self-generating, and the protective film is completely destroyed [4]. The severity of corrosion is dependent on a variety of factors, most notably, temperature, chloride content, and pH [5]. This study examined corrosion behavior at room temperature (25°C) and 3.5 wt% NaCl (sea water salt concentration) in solutions of pH 7, 9, and 12.

The high possibilities of general and pitting corrosion advocate methods of carbon steel surface treatment to combat the issue. Numerous coating techniques exist in efforts to prevent corrosion and prolong the lifespan of alloys. While chromate conversion coatings (CCCs) have proven successful in limiting corrosion when applied, these coatings can be threatening to the environment due to their carcinogenic nature of application [6]. A viable alternative lies in the use of non-toxic, eco-friendly, organopolysiloxane precursors as sol-gel coating films. Two precursors: methacryloxypropyltrimethoxysilane (MAPTMS) and tetraethylorthosilicate (TEOS) have demonstrated superb corrosion protection when used in alloy surface treatment. Rosero-Navarro describes the anticorrosive protection and self-healing properties of a MAPTMS + TEOS sol-gel coating when applied to AA2024 alloys [7]. Gelling and Galván showed that preparation of a hybrid sol-gel film in a 2:1 MAPTMS, TMOS (tetramethylorthosilicate) molar ratio provided the highest degree of corrosion protection for AA2024 alloys [2]. Limited studies exist for the corrosion protection of carbon steel alloys using sol-gel films. The research and testing performed in this study aimed to verify whether increased corrosion protection would be exhibited by MAPTMS + TEOS sol-gel treated AISI 1008 carbon steel.

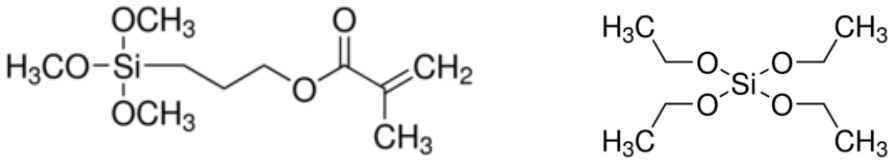

Figure 1. The structural formulas of MAPTMS (left) and TEOS (right)

The addition of corrosion inhibitors into the sol-gel film network has also confirmed a promising approach for improving the corrosion protection performance of various alloys. Corrosion inhibitors work by binding to the polar surface of the metal, acting as a barrier to charge transfer (inhibiting the anodic and cathodic corrosion reactions). Mennucci and Banczek showed that benzotriazole (BTA) could be used as an effective corrosion inhibitor for reinforced steel in concrete in 3.5 wt% NaCl solutions [8]. Selvi and Raman showed that the use of BTA as a corrosion inhibitor increased charge transfer resistance and lowered corrosion current density for carbon steel in mildly acidic media [9]. BTA acts as a mixed inhibitor, slowing the rate of anodic and cathodic reactions [10]. It is anticipated that the inclusion of BTA into the sol-gel mixture could provide additional corrosion protection by means of physical entrapment into the porous networks of the sol-gel coating [2]. The primary testing goal was to investigate the corrosion behavior of unmodified sol-gel coatings and BTA modified sol-gel coatings compared to blank AISI 1008 carbon steel samples at room temperature in NaCl solutions of varying pH.

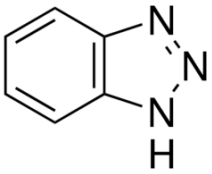

Figure 2. The structural formula of benzotriazole (BTA)

Experimental Methods

Materials: AISI 1008 carbon steel samples were used as the working electrodes within a three-electrode cell in every experiment. The following table shows the chemical composition of the tested carbon steel.

Table 1. AISI 1008 Carbon Steel Elemental Composition (wt%)

Element	Content (%)
Iron, Fe	bal.
Manganese, Mn	0.5
Carbon, C	0.1
Sulfur, S	0.05
Phosphorous, P	0.04

The steel was cut into thin, square strips and embedded in a non-conductive, acrylic resin. A conductive wire was taped to the samples before mounting, which protruded outward from the resin (Figure 3). Prior to the beginning of each experiment, samples were wet ground from 300 to 1200 silicon carbide grit paper, rinsed with ethanol, and air dried before immersion into solution. The edges of the steel were painted with a thin coating of stop-off lacquer to limit exposed area and prevent crevice corrosion of the samples. A surface area of approximately $1\ cm^2$ was exposed to the electrolyte per sample.

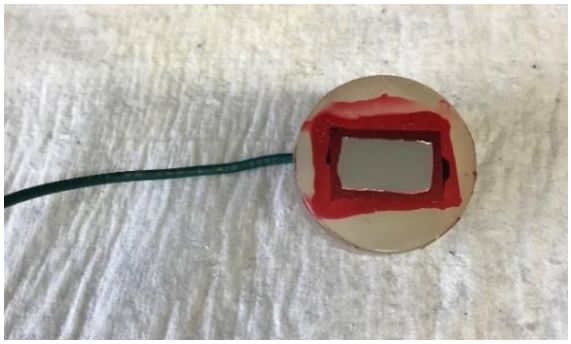

Figure 3. Mounted Sample; Epoxy resin encompassed the AISI 1008 carbon steel with a thin coating of stop-off lacquer to limit area and prevent crevice corrosion.

Unmodified Sol-Gel Films: The initial sols were prepared by co-hydrolysis and polycondensation of methacryloxypropyltrimethoxysilane (MAPTMS) and tetraethylorthosilicate (TEOS). MAPTMS and TEOS were combined in 2:1 molar ratios. Deionized water and ethanol were added with a MAPTMS+TEOS/water/ethanol molar ratio of 1:3:3. The initial mixture was magnetically stirred at room temperature for 12 hours.

Benzotriazole Modified Sol-Gel Films: Benzotriazole (BTA) was added to the MAPTMS/TEOS/water/ethanol mixture in a ratio of 1 gram per 25 ml of unmodified sol-gel solution. The resulting mixture was magnetically stirred at room temperature for 12 hours.

Spin Coating: Each sol-gel film was applied using a *12A Super Spin Coater*. Mounted samples were placed on the center of the device where the sol-gels were applied dropwise as the samples were spun. A spin rate of 100 rpm for 10 seconds followed by 500 rpm for 10 seconds was used. Twenty droplets of unmodified sol-gel and fifteen droplets of BTA-modified sol-gel were applied to two separate samples. The BTA modified sol-gel produced a more viscous solution where applied droplets were higher in volume, thus less droplets were used for coating application. Following the coating application, unmodified sol-gel samples were dried at 80°C for 2 hours.

BTA-modified sol-gel samples required a longer drying time in order for the coating to solidify properly, and thus were dried at 80°C for 3 hours. A thin and even, transparent coating was observed for the unmodified sol-gel and the BTA-modified sol-gel post drying.

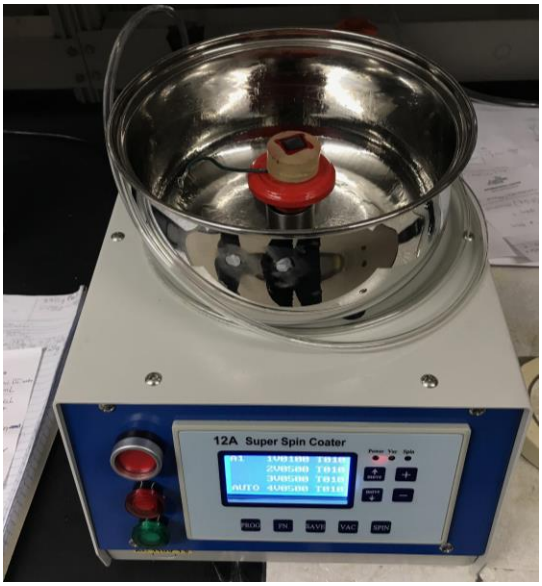

Figure 4. A photo image of a mounted sample placed on a *12A Super Spin Coater* that was used to coat a thin layer of sol-gel coating to the sample.

Table 2. Sol-Gel Preparation Details

Sample	Unmodified sol-gel	BTA modified sol-gel
MAPTMS:TEOS molar ratio	0.084027778	0.084027778
MAPTMS+TEOS:H2O:EtOH molar ratio	0.043784722	0.043784722
BTA: MAPTMS+TEOS+H2O+EtOH mass ratio	-	1g:25 ml
Stirring time	12 hrs at RT	12 hrs at RT
Droplets applied for coating	20	15
Dry time	2 hrs at 80°C	3 hrs at 80°C

FTIR Spectroscopy: Prior to electrochemical testing, coated samples were analyzed under FTIR spectroscopy. Larger sheet samples were spin coated with various sol gels and dried following the same procedure previously described. Each coated sample along with a blank, control sample

were placed into the spectrometer. 48 scans were performed for each sample and the resulting spectroscopies were saved for analysis.

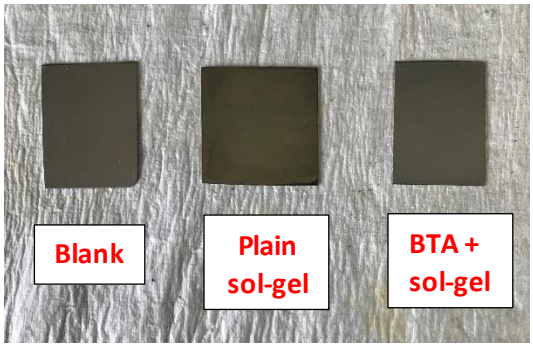

Figure 5. The appearance of the samples: plain steel, steel coated with plain (unmodified) sol-gel, and steel coated with sol-gel containing BTA used for FTIR analysis.

Solution Preparation: Three solutions were prepared as mediums for testing. A simulated pore solution of saturated calcium hydroxide (pH 12) was prepared by adding 0.5 grams of calcium hydroxide to 500 ml of deionized water. A carbonate-bicarbonate buffer solution (pH 9) was prepared by adding 0.47 grams of sodium carbonate along with 3.8 grams of sodium bicarbonate to 500 ml of deionized water. Pure deionized water (pH 7) was used as a third solution. Sodium chloride (NaCl) was added in 3.5 wt% to each solution. The addition of NaCl was performed to examine possible pitting behavior in higher pH solutions.

Table 3. Solution Preparation Details

Solution	Contents	NaCl (wt%)
Simulated pore (sat. Ca(OH)2)	0.5 g Ca(OH)2 + 500 ml DI water	3.5
Carbonate-bicarbonate buffer	0.47 g Na2CO3 + 3.8 g NaHCO3 + 500 ml DI water	3.5
Deionized water	500 ml DI water	3.5

Electrochemical Testing Techniques: A *Gamry Instruments Reference 600 Potentiostat* was utilized to conduct electrochemical testing. The working electrodes (carbon steel samples) were

used in a three-electrode cell comprised of a saturated calomel reference electrode (SCE) and a graphite rod counter electrode. Corrosion behavior of the specimens were analyzed through a series of three tests: Open Circuit Potential (OCP), Potentiostatic EIS, and Cyclic Polarization. Each of the three tests were performed in the same solution, back-to-back in this order. The initial OCP test allowed the sample to reach its resting potential in solution over the course of one hour. The Potentiostatic EIS test applied an alternating current (AC) voltage of 10 mV r.m.s. at 10 points/decade and at OCP. An initial frequency of 100,000 Hz was applied which slowed to 0.01 Hz by the end of the test. The Cyclic Polarization test scanned applied potential from -0.2 V_{SCE} to 0.2V_{SCE} with an apex current of 25 mA/cm^2. Following the set of tests, samples were removed, rinsed with deionized water, and reground to be coated and tested again. Used solution was disposed of appropriately. Three series of tests were performed in each solution for blank carbon steel, sol-gel coated carbon steel, and BTA modified sol-gel coated carbon steel to accurately verify results. Results for each test were saved for research and analysis.

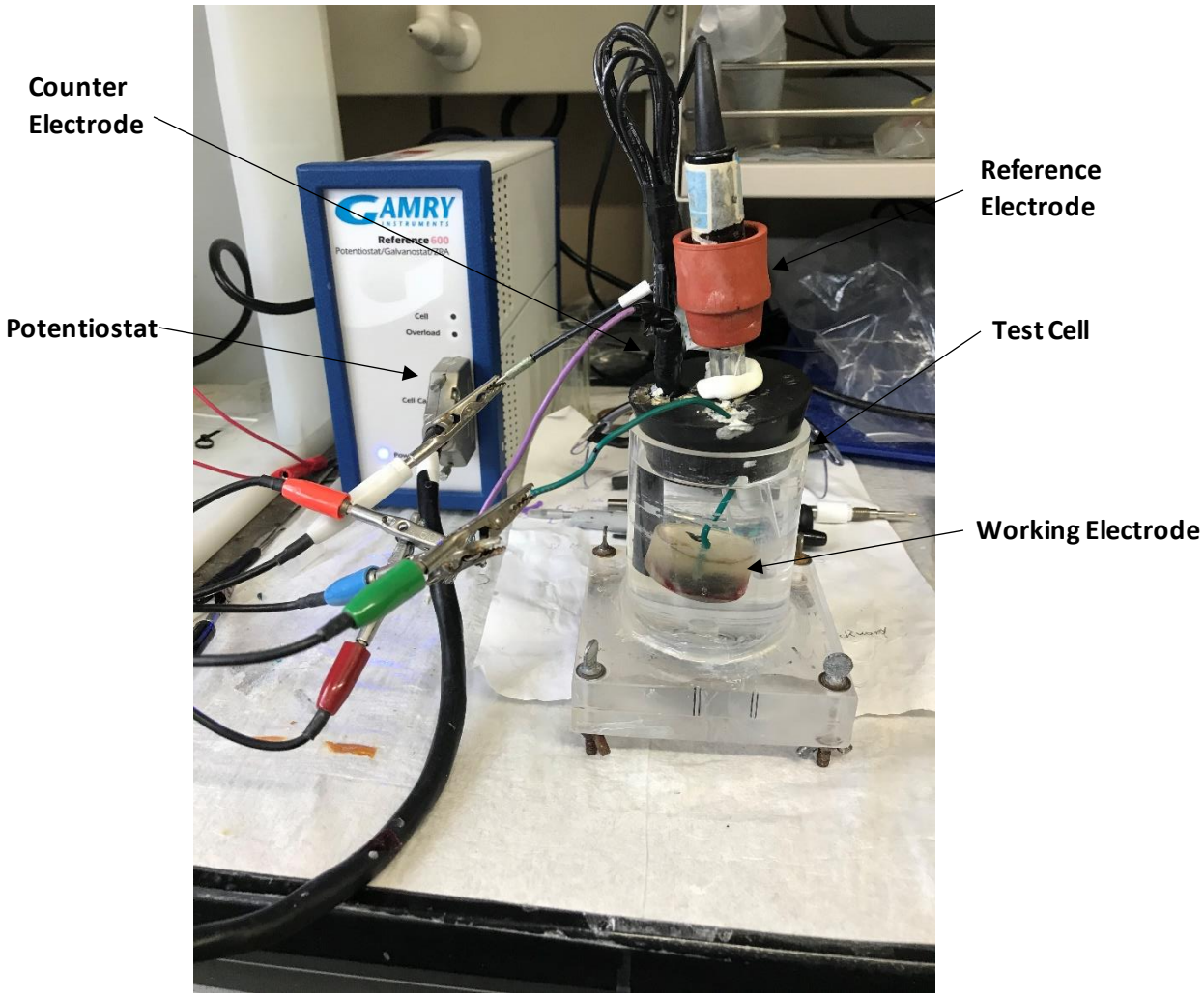

Figure 6. Electrochemical Cell Set-up containing three electrodes connected to a potentiostat

Laboratory Safety

Numerous safety precautions were taken throughout the completion of testing. Due to COVID-19 regulations in the laboratory during the time of testing, gloves and face coverings were worn, and social distancing took place at all times. Hands were washed as frequently as possible to slow the spread of germs. Specific to experimental procedures, all testing solutions were covered with parafilm and placed under the laboratory hood. Flammable chemicals including MAPTMS and TEOS were stored in a separate, fire-proof cabinet. Electrochemical tests were disconnected

immediately following completion, while test solutions were disposed of properly. When polishing samples, the machine was calibrated properly, and safety gloves were worn to prevent cuts/scrapes. When using the oven to dry samples, oven mitts were used to avoid burns when inserting and removing samples. Lastly, fire extinguishers and chemical showers were located in the lab for use in case of emergency.

Regulations/Standards

All electrochemical testing was performed according to ASTM G3-14 - Standard Practice for Conventions Applicable to Electrochemical Measurements in Corrosion Testing. All outlets from the potentiostat were connected correctly with alligator clips to the working, reference, and counter electrodes. Tests were monitored throughout duration to verify a continuous good connection between the potentiostat and the electrodes. Each electrode was rinsed with deionized water at the conclusion of each test, and solutions were disposed of properly. FTIR spectroscopy testing was carried out in accordance with ASTM E2412 - Infrared Organic Spectrometry (FTIR). The sol-gel coating on each sample was checked to be uniform and homogeneous before loading into the device. A force of 75 N was applied for the FTIR scan, and samples were preserved in plastic baggies following testing. Overall, each standard was closely followed to insure accurate and safe testing procedure and analysis.

Testing Budget

All testing was completed in the University of Akron Engineering Research Center where the use of the lab was free to research students, thus labor costs will not be taken into consideration for this section. In addition, use of computers for analyzing and modeling data were not included in

the budget. Listed in Table 4 are the costs of materials/equipment and chemicals for the full completion of testing. The total project cost equated to $24,384.

Table 4. Materials/Equipment/Chemicals and Prices for Testing

Materials/Equipment/Chemicals	Cost ($)
Gamry Reference 600 Potentiostat	10,000
12A Super Spin Coater	2,000
FTIR Spectrometer	5,000
Graphite Rod Counter Electrode	200
SCE Reference Electrode	125
Carbon Steel Samples	50
Polish Wheel	4,000
300-1200 Grit Sandpaper	40
Drying Oven	2,000
200 ml Test Cell	30
MAPTMS	96
TEOS	63
BTA	46
Ethanol	82
Sodium Chloride	15
Calcium Hydroxide	11
Sodium Bicarbonate	12
Sodium Carbonate	14
Lab PPE	100
Miscellaneous Lab Equipment	500
Total ($)	**24,384**

Data and Results

Characterization of Unmodified and BTA Modified Sol-Gel Films: The preparation of the organopolysiloxane precursors (MAPTMS and TEOS) along with BTA produced a homogenous, transparent solution. Coatings were applied evenly and covered the entire surface area of the substrate. The presence of the sol-gel films was verified by FTIR spectroscopy shown in Figure 7.

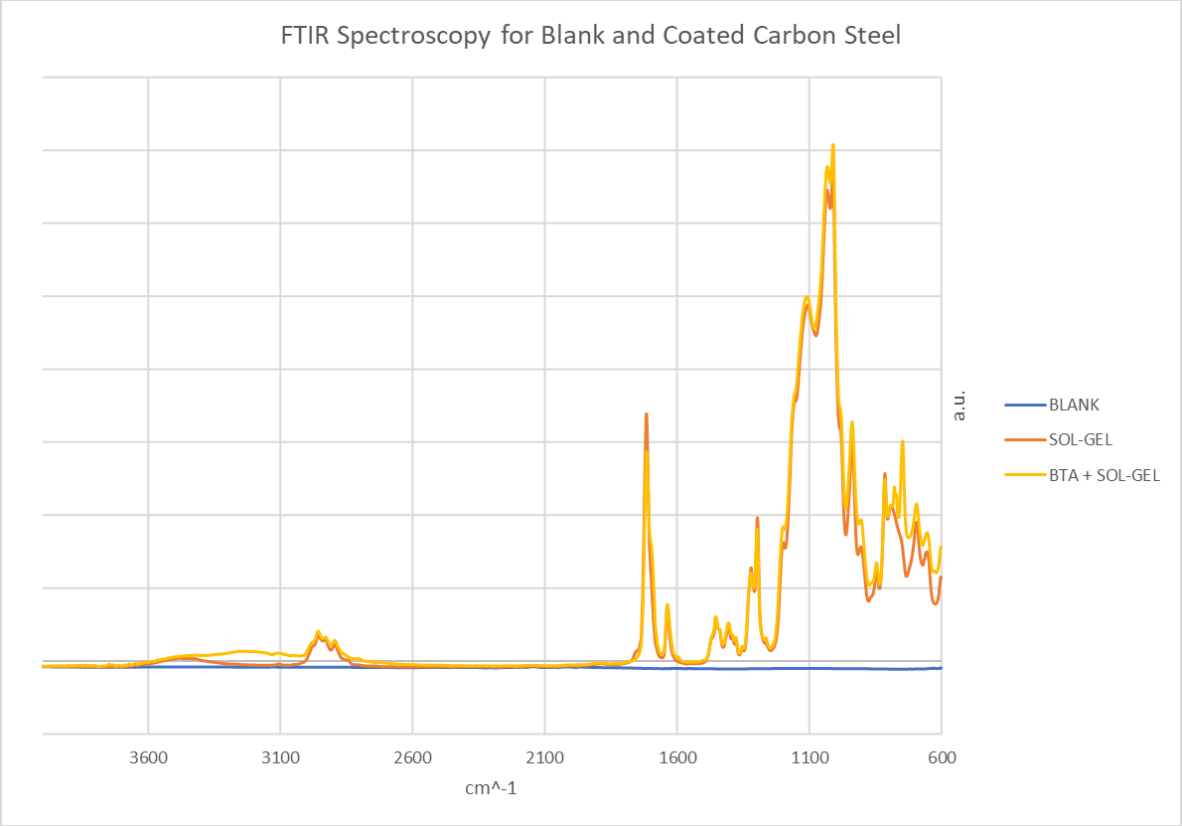

Figure 7. FTIR Spectroscopy for Blank and Coated Carbon Steel; C-H, C-O, and C-C bonds in MAPTMS and TEOS are evident from large peaks at ~2900, ~1700, and ~1000 cm^{-1}, respectively. A higher peak observed from BTA modified sol-gel coated carbon steel at ~1000 cm^{-1} correlates to C-N bonding exhibited in BTA. Lastly, a slight peak around 3200 cm^{-1} is evident of a N-H bond in BTA.

The confirmation of sol-gel coating presence and characterization allowed for substantiated analysis of electrochemical results. All electrochemical results were viewed and modelled using *Gamry Echem Analyst* (see Appendices).

OCP Measurements: Prior to EIS and CPP, OCP measurements were taken to allow the system to reach steady state. At the conclusion of the test, a stable, open circuit potential was identified for each carbon steel sample in varying solution. OCP was crucial such that EIS and CPP tests could

be completed in steady state conditions. An example of OCP data in pH 12 solution is shown in Figure 8, below.

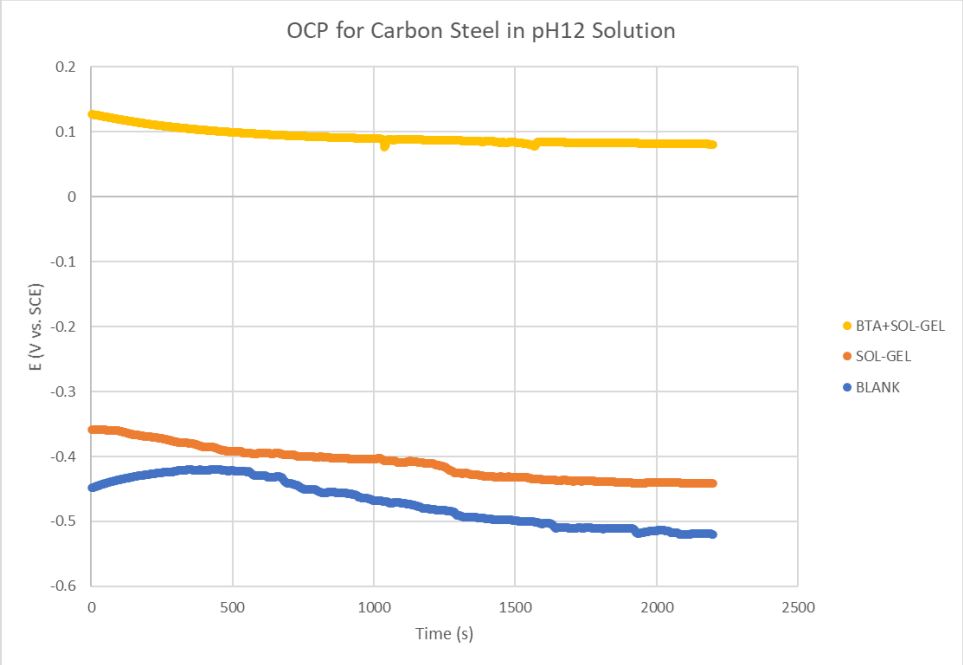

Figure 8. OCP for Carbon Steel in pH 12 Solution; the potentials see a higher variance initially, but level out to constant values by the end of the test. OCP was highest for BTA modified sol-gel coated carbon steel, in the middle for sol-gel coated carbon steel, and lowest for blank carbon steel.

EIS Measurements: The data generated from EIS provided Nyquist plots for blank, sol-gel coated, and BTA modified sol-gel coated carbon steel. Nyquist plots show the relationship between real impedance and imaginary impedance over the broad range of frequency, usually producing a semi-circle of data points. This data can further be modelled according to an equivalent electric circuit (EEC) which describes the nature of the corrosion reaction within the system. Two different EECs were used to model EIS data shown in Figure 9.

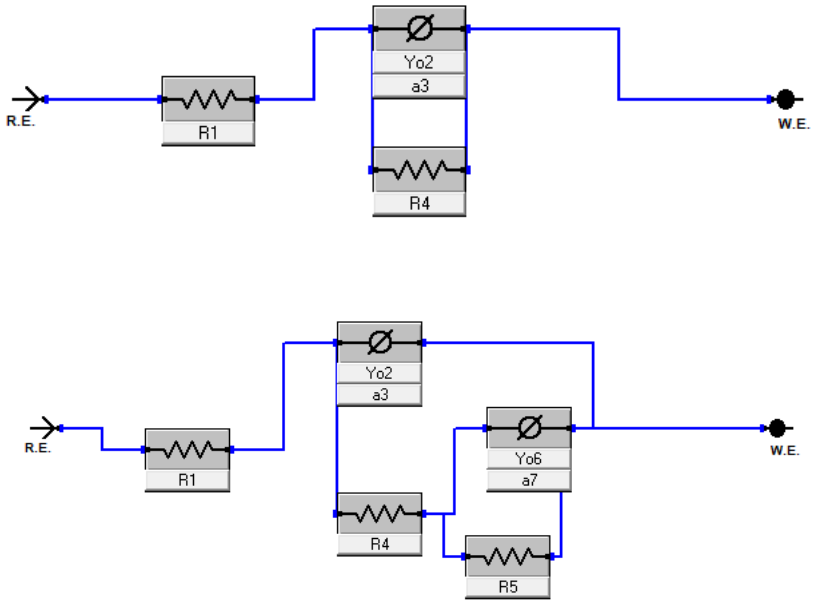

Figure 9. EECs for Blank (top) and Sol-Gel Coated/BTA Modified Sol-Gel Coated Carbon Steel (bottom)

Each EEC consisted of a combination of resistors and capacitors. The models contained constant phase elements (CPE) instead of capacitors to account for non-ideal capacitance attributed to surface heterogeneities in the carbon steel samples [11]. Polarization resistance was the main element focused on as this parameter described the sample's resistance to corrosion in the system. Polarization resistance was denoted as R4 and R4 + R5 in the blank and sol-gel coated/BTA modified sol-gel coated EECs, respectively. Each model was chosen based on the expected elements contained in the system and goodness of fit produced in the model. Nyquist plots are provided below, showing the effect of solution pH on the polarization resistance of blank, sol-gel coated, and BTA modified sol-gel coated carbon steel. The resistance to corrosion can be estimated by the diameter of the Nyquist semicircle observed in the plot.

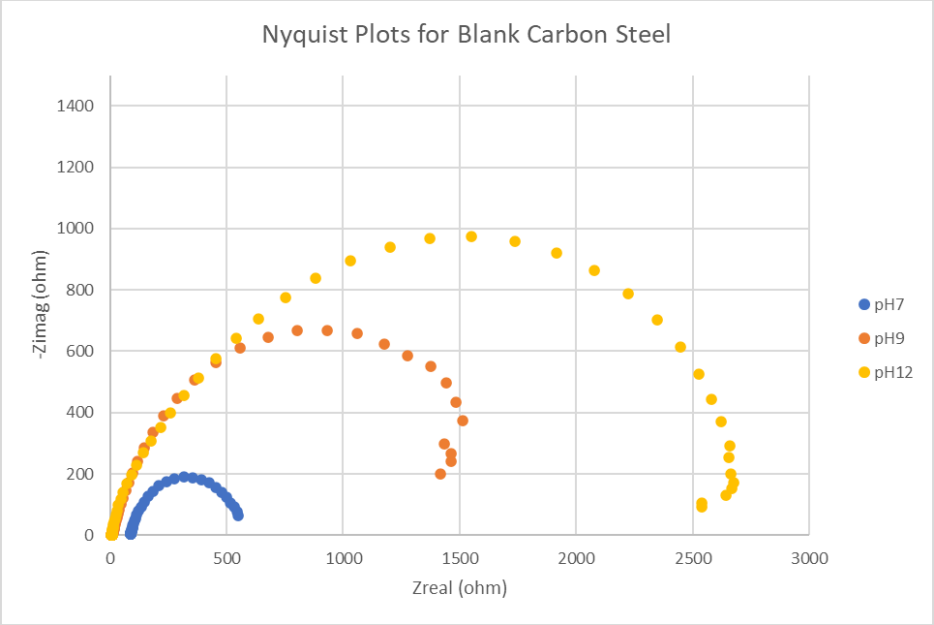

Figure 10. Nyquist Plot for Blank Carbon Steel (3.5 wt% NaCl); an increase in polarization resistance is observed as pH increases from 7 to 12.

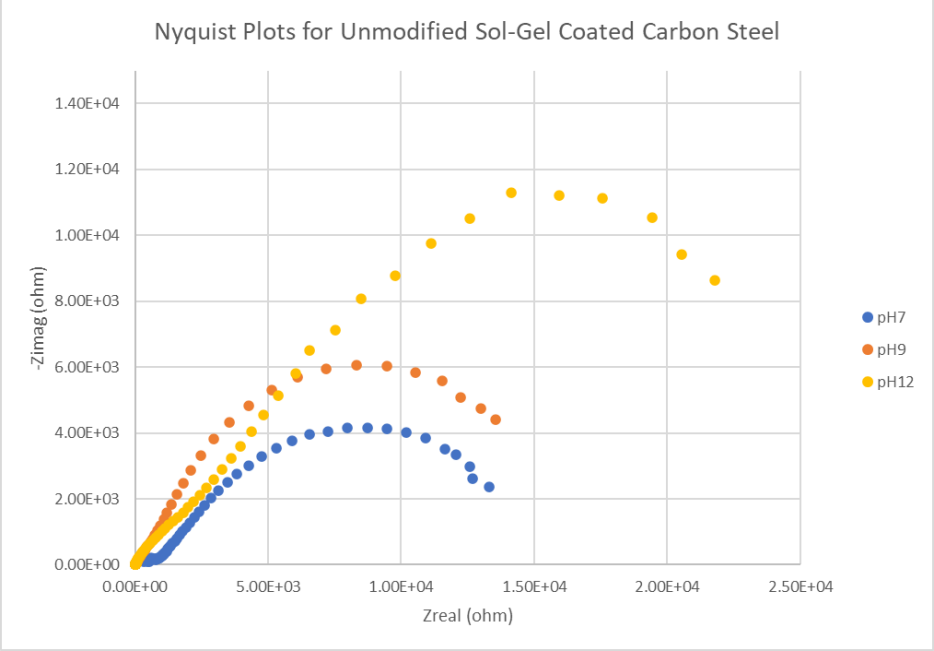

Figure 11. Nyquist Plot for Sol-Gel Coated Carbon Steel (3.5 wt% NaCl); an increase in polarization resistance is observed as pH increases from 7 to 12. A noticeable increase in polarization resistance occurred for sol-gel coated carbon steel when compared to blank samples.

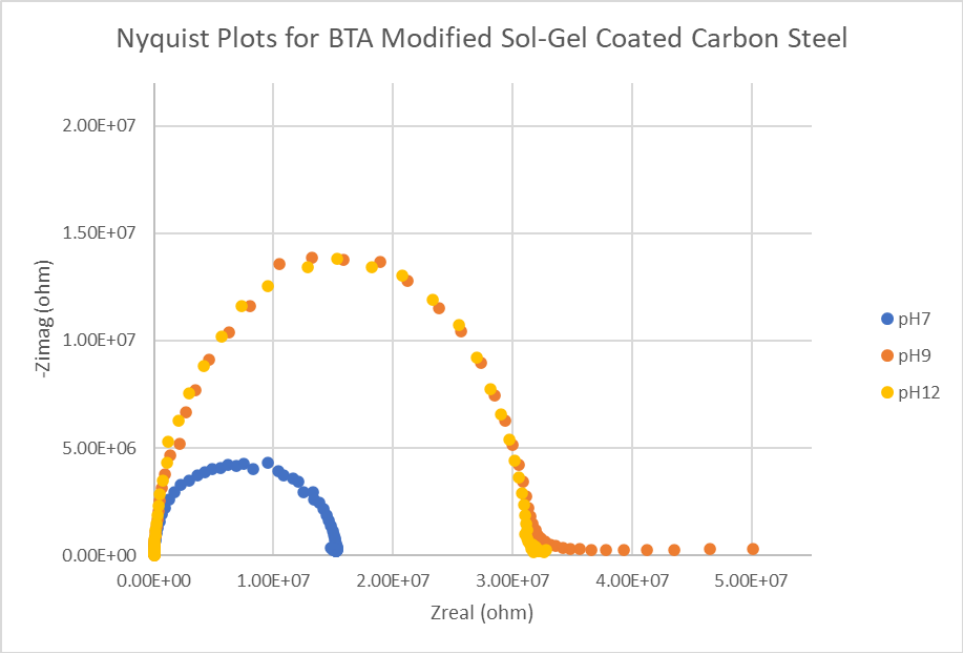

Figure 12. Nyquist Plot for BTA Modified Sol-Gel Coated Carbon Steel (3.5 wt% NaCl); an increase in polarization resistance is observed as pH increased from 7 to 9, but a decrease occurred from 9 to 12. A drastic increase in polarization resistance (nearly three magnitudes) occurred for BTA modified sol-gel coated carbon steel compared to blank and sol-gel coated samples.

CPP Measurements: Cyclic polarization curves were generated for blank, sol-gel coated, and BTA modified sol-gel coated carbon steel. Corrosion current density (icorr) and corrosion potential (Ecorr) were determined through Tafel fits based on the anodic (positive) and cathodic (negative) slopes of the curves. An example Tafel fit is shown in Figure 13.

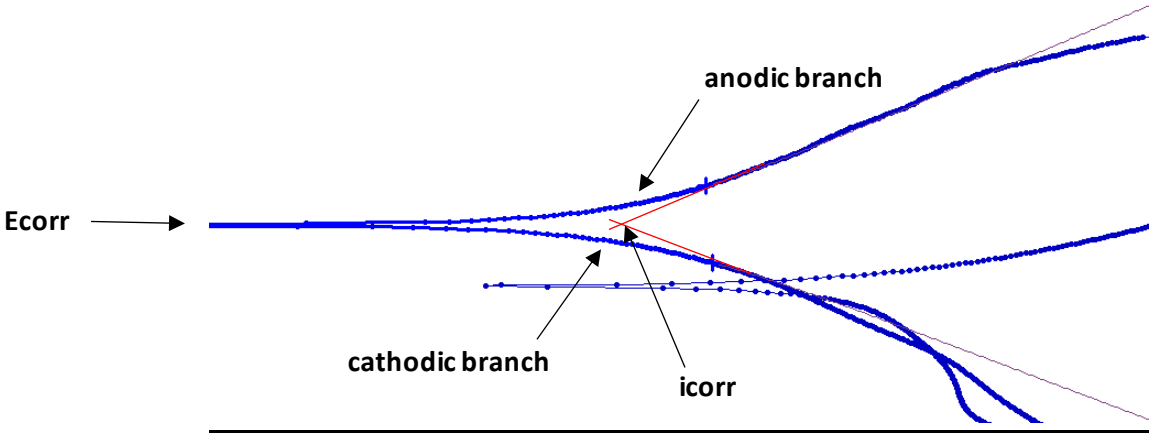

Figure 13. Tafel Fit for Sol-Gel Coated Carbon Steel in pH 12 Solution; Ecorr and icorr are determined from the intersection of the anodic and cathodic branches.

Cyclic polarization curves are provided below, showing the effect of solution pH on icorr and Ecorr of blank, sol-gel coated, and BTA modified sol-gel coated carbon steel.

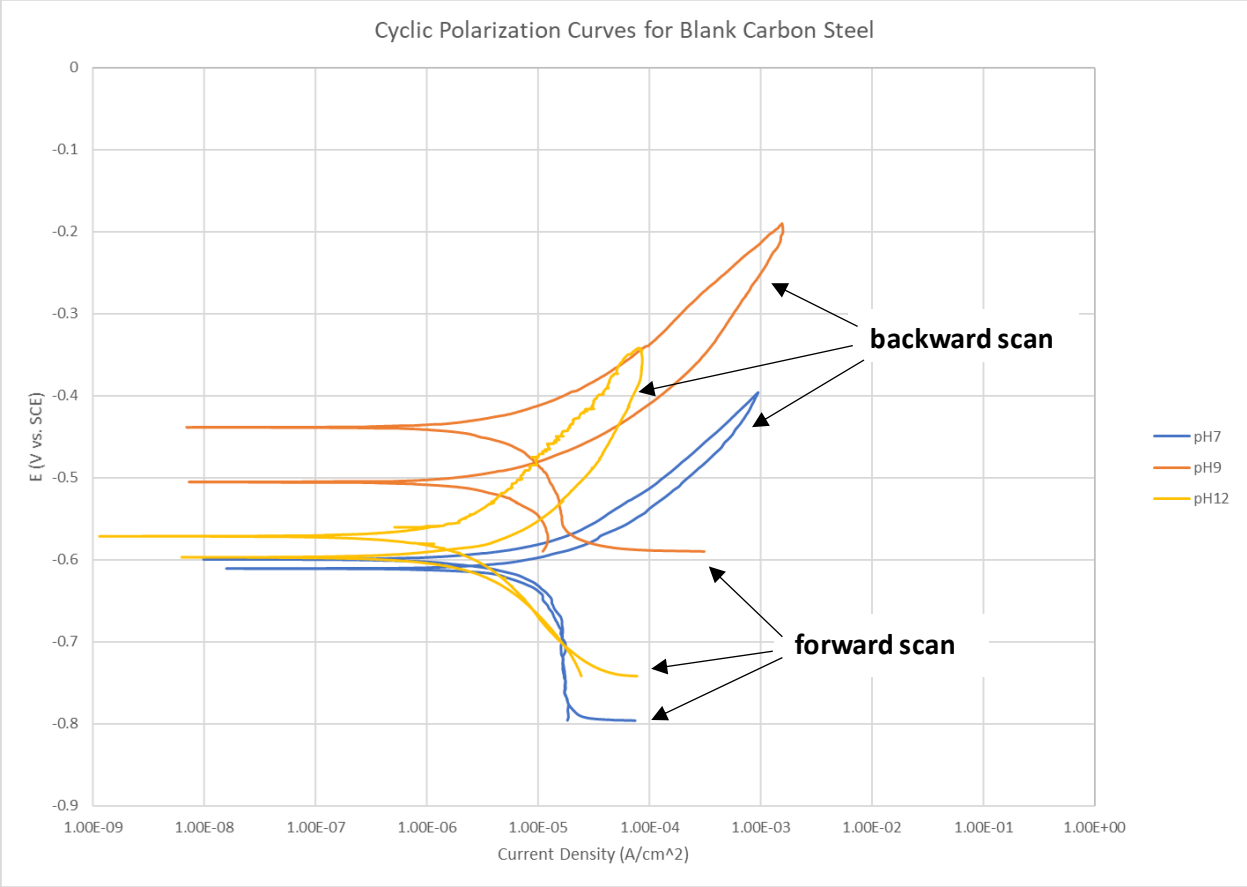

Figure 14. Cyclic Polarization Curves for Blank Carbon Steel (3.5 wt% NaCl); icorr decreased from pH 7 to 9 but increased slightly from pH 9 to 12. Likewise, Ecorr increased from pH 7 to 9 but decreased from pH 9 to 12. Larger positive hysteresis loops for the backward scan were observed in higher pH solutions suggesting higher damage (with possibility of pitting) following polarization.

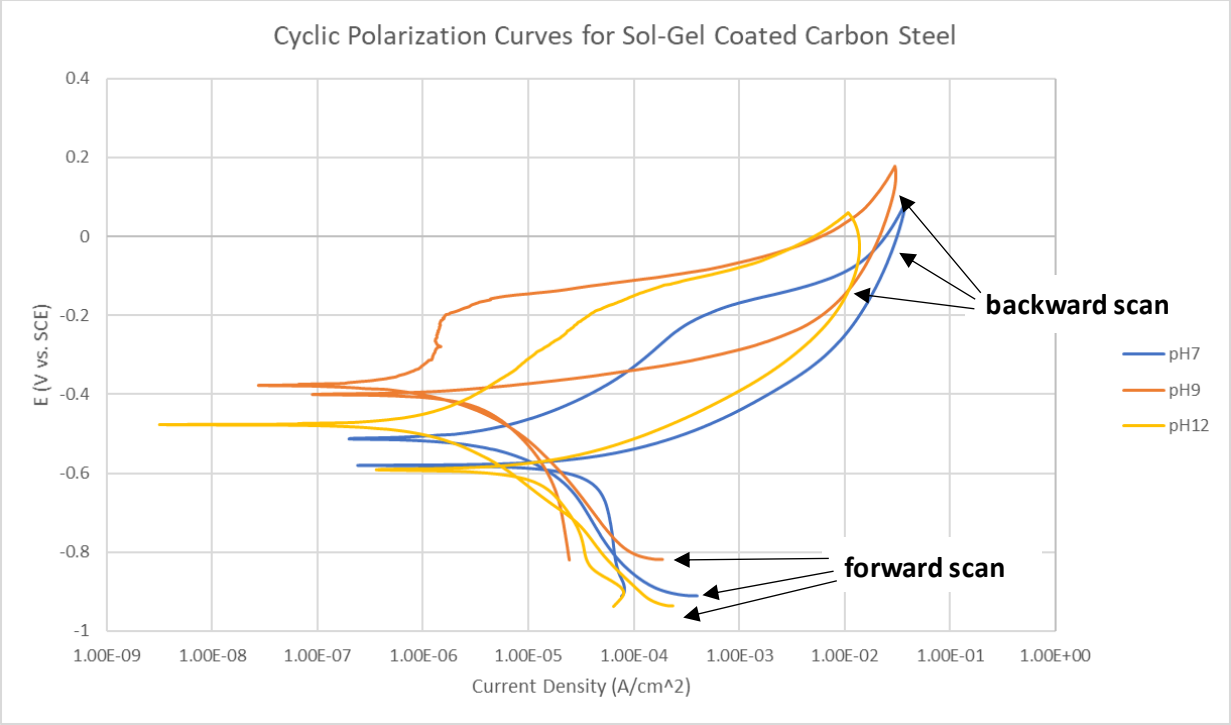

Figure 15. Cyclic Polarization Curves for Sol-Gel Coated Carbon Steel (3.5 wt% NaCl); i_{corr} decreased from pH 7 to 9 but increased slightly from pH 9 to 12. Likewise, E_{corr} increased from pH 7 to 9 but decreased from pH 9 to 12. Larger positive hysteresis loops for the backward scan were observed in higher pH solutions suggesting damage to the sol-gel film (with possibility of pitting) following polarization.

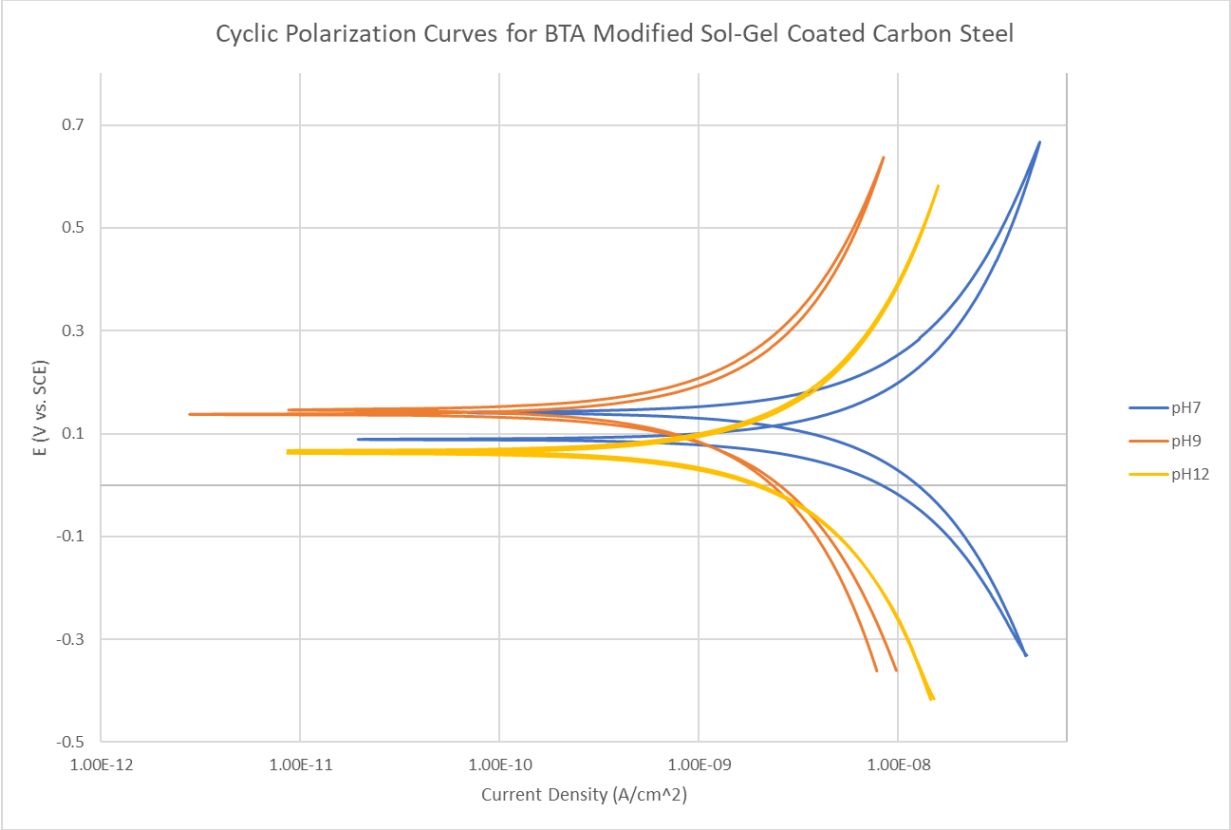

Figure 16. Cyclic Polarization Curves for BTA Modified Sol-Gel Coated Carbon Steel (3.5 wt% NaCl); icorr decreased from pH 7 to 9 but increased slightly from pH 9 to 12. Likewise, Ecorr increased from pH 7 to 9 but decreased from pH 9 to 12. Ecorr was significantly higher and icorr was significantly lower for BTA modified sol-gel coated carbon steel when compared to sol-gel coated and blank samples. Larger positive hysteresis loops for the backward scan were observed in lower pH solutions suggesting a lower susceptibility of damage to the BTA modified sol-gel film at higher pHs following polarization.

Discussion/Analysis

It is evident from the Nyquist plots **(Figures 10-12)** that pH 7 solutions exhibited the lowest resistance to polarization when compared to higher pHs. The increase in polarization resistance from pH 7 to pH 9 and 12 was particularly evident in BTA modified sol-gel coated carbon steel. This trend is justified as the pKa of BTA is 8.37 meaning the molecule will act as a weak acid in lower pH solutions [12]. While polarization resistance for pH 12 solutions also outperformed pH

9 for blank and sol-gel coated carbon steel, polarization resistance slightly decreased from pH 9 to 12 for BTA modified sol-gel coated carbon steel. This slight decrease could be due to carbonates (in pH 9 solution) filling and protecting pores [13]; however, the difference in corrosion current density is very minimal. Overall, polarization resistance increased in pH 9 and 12 solutions compared to pH 7 due to formation of a protective oxide film [14].

Cyclic polarization curves **(Figures 14-16)** show that corrosion current density was highest for pH 7 solutions in blank, sol-gel coated, and BTA modified sol-gel coated carbon steel. BTA modified sol-gel coated samples obtained a drastically lower icorr when compared to sol-gel coated and blank carbon steel. Corrosion current density generally decreased as solution pH increased with a few, slight discrepancies in sol-gel coated and BTA modified sol-gel coated samples. Much like polarization resistances obtained from EIS, a slightly higher corrosion current density was observed in pH 12 solutions compared to pH 9 for sol-gel coated and BTA modified sol-gel coated carbon steel. Once again, the difference was very slight and did not affect any major conclusions. It should be noted that hysteresis loops increased with higher pH during the backward scan for blank and sol-gel coated carbon steel. These results can be attributed to slight destruction of passive films and pitting corrosion at higher pH [15]. However, the opposite trend was observed for BTA modified sol-gel coated carbon steel. Hysteresis loops likely decreased as pH increased for BTA modified sol-gel coated samples due to higher corrosion inhibition of BTA in higher pH solutions.

When comparing corrosion data obtained from electrochemical testing, the improved performance of the sol-gel coated and BTA modified sol-gel coated samples can be clearly observed. Table 5 contains icorr, Ecorr, and Rp for each sample in pH 7, 9, and 12 solutions.

Table 5. Electrochemical Parameter Data

	Solution pH	icorr-µA (CPP)	Ecorr-mV/SCE (CPP)	Rp-ohm (EIS)
Blank	7	10.4	-611	601
	9	7.3	-438	1,635
	12	2.6	-571	2,655
Sol-Gel	7	9.3	-512	12,590
	9	1.4	-489	16,730
	12	1.5	-498	27,610
BTA+Sol-Gel	7	0.004	98	7,458,000
	9	0.00071	112	18,800,000
	12	0.00097	74	15,900,000

Corrosion current density for sol-gel coated samples was slightly lower when compared to blank carbon steel, while corrosion potential was slightly more positive (with the exception of pH 9). Polarization resistance saw a more drastic change, increasing by roughly one magnitude. From this comparison it can be determined that the presence of the sol-gel film increased corrosion protection of carbon steel. When comparing BTA modified sol-gel coated samples to both sol-gel coated and blank samples, the difference in corrosion parameters is immense. There is roughly a three order of magnitude difference in icorr and Rp between sol-gel coated and BTA modified sol-gel coated samples, with the BTA tremendously increasing corrosion performance. Corrosion potential was also observed to be much more positive in the comparison. Thus, the presence of BTA as a corrosion inhibitor in the sol-gel matrix enormously improved overall corrosion protection. Figure 17 shows a comparison in polarization curves for blank, sol-gel coated, and BTA modified sol-gel coated carbon steel samples in pH 12 solution.

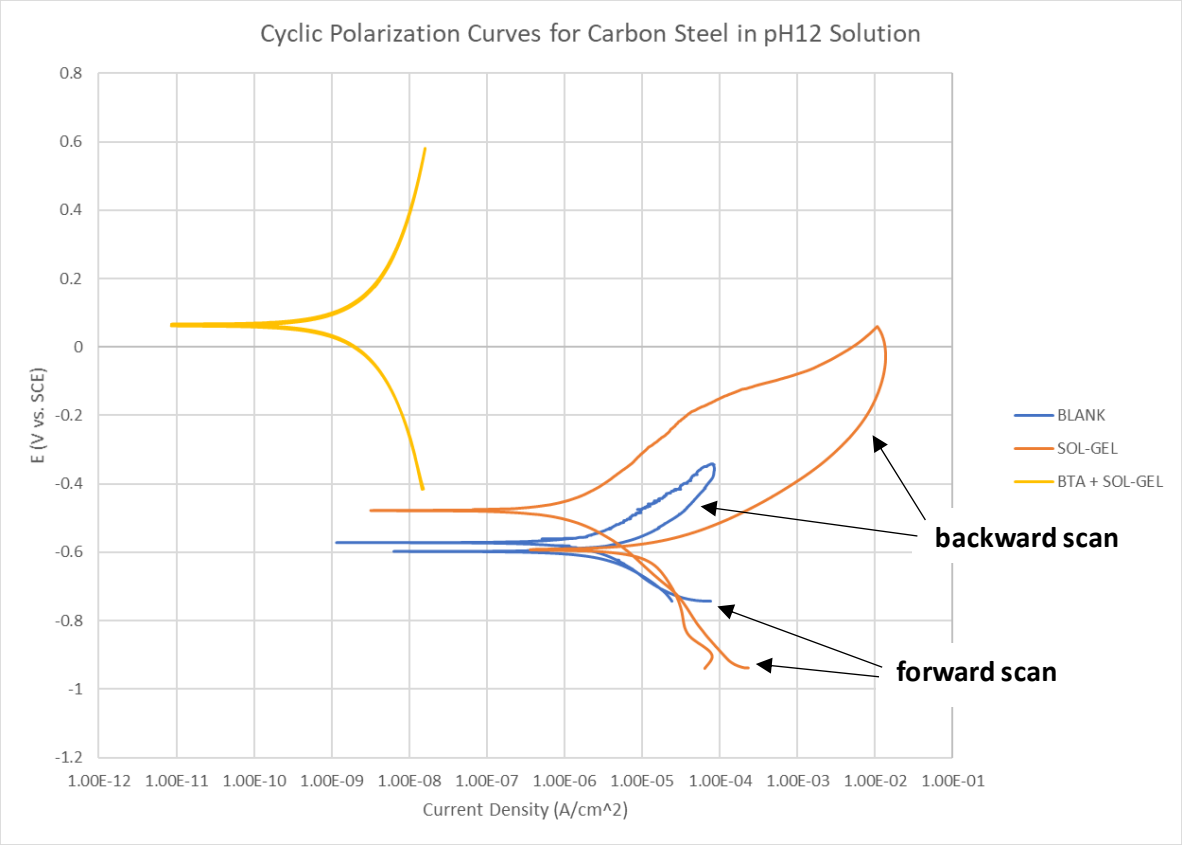

Figure 17. Cyclic Polarization Curves for Blank and Coated Carbon Steel in pH 12 Solution; corrosion current density only slightly decreases between blank and sol-gel coated samples but immensely decreases between sol-gel coated and BTA modified sol-gel coated samples.

Corrosion current densities obtained from each Tafel fit were used to find corrosion rate (mm/yr) using equation 7. Corrosion rates computed from EIS were not discussed in this section as the Tafel fits from CPP provided a more accurate analysis. Table 6 shows corrosion rates for each sample in varying pH solution while Figure 18 provides a graphical representation of the comparison.

$$CR\left(\frac{mm}{yr}\right) = 0.00327 * icorr\left(\frac{\mu A}{cm^2}\right) * \left(\frac{E_w}{\rho}\right) \quad (7)$$

Table 6. Corrosion Rate Data (CPP)

	Solution pH	CR (mm/yr)
Blank	7	0.12064846
	9	0.08468594
	12	0.03016211
Sol-Gel	7	0.10788756
	9	0.01624114
	12	0.01740122
BTA+Sol-Gel	7	4.6403E-05
	9	8.2366E-06
	12	1.1253E-05

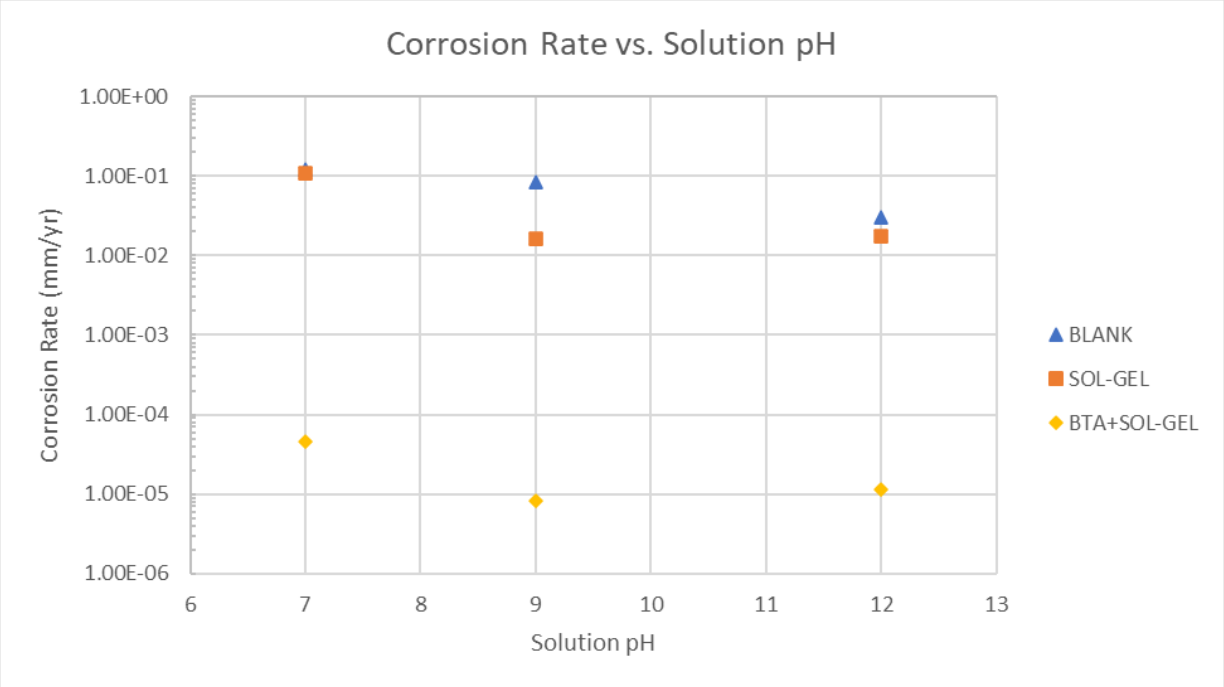

Figure 18. Corrosion Rates vs. Solution pH for Blank, Sol-Gel Coated, and BTA Modified Sol-Gel Coated Carbon Steel

While unmodified sol-gel coated carbon steel showed a slight increase in corrosion performance over blank samples, the degree of improvement was not as high as expected. Figure 17 shows that

the sol-gel film does outperform the blank sample; however, the film becomes partially destructed following polarization. It is evident from Figure 18 that the addition of BTA into the sol-gel matrix had the biggest impact on corrosion rate. The presence of BTA was most effective in the molecule's ability to bind to the metal surface (through N atoms) while entrapped in the sol-gel, greatly decreasing the ability for charge transfer in the system [16]. Thus, the incorporation of BTA into sol-gel films is highly recommended for the corrosion protection of AISI 1008 carbon steel.

Further testing is recommended to confirm the results presented in this study. Experimental error was possible in some cases where the potentiostat lost connection. Different molar ratios of MAPTMS and TEOS for sol-gel preparation should be experimented with, along with different amounts of BTA added to the sol-gel matrix. Different concentration of NaCl could be used in addition to a higher range of pH solutions. Lastly, SEM/XRD could be used prior to electrochemical testing for characterization of the sol-gel films, and post electrochemical testing to clearly identify specimen damage, pitting, corrosion products, etc. Aside from these possible improvements, the triplicate testing that was performed allowed for a reliable analysis of electrochemical results.

Intellectual Property

In this study, samples were coated two dimensionally using a *12A Super Spin Coater*. However, in order to effectively coat reinforced steel for concrete infrastructure, a three-dimensional coating application is required. This makes the use of spin coating unsuitable for real world applications as this technique is not feasible for three-dimensional coatings. Instead, a method of "dip coating" for reinforced steel is proposed. Faustini and Louis showed how corrosion protection of substrates

was increased through a dip coating process with sol-gel films [17]. A simplified, dip coating model, named *Rebar Coater*, illustrates the coating process for reinforced steel (Figure 19).

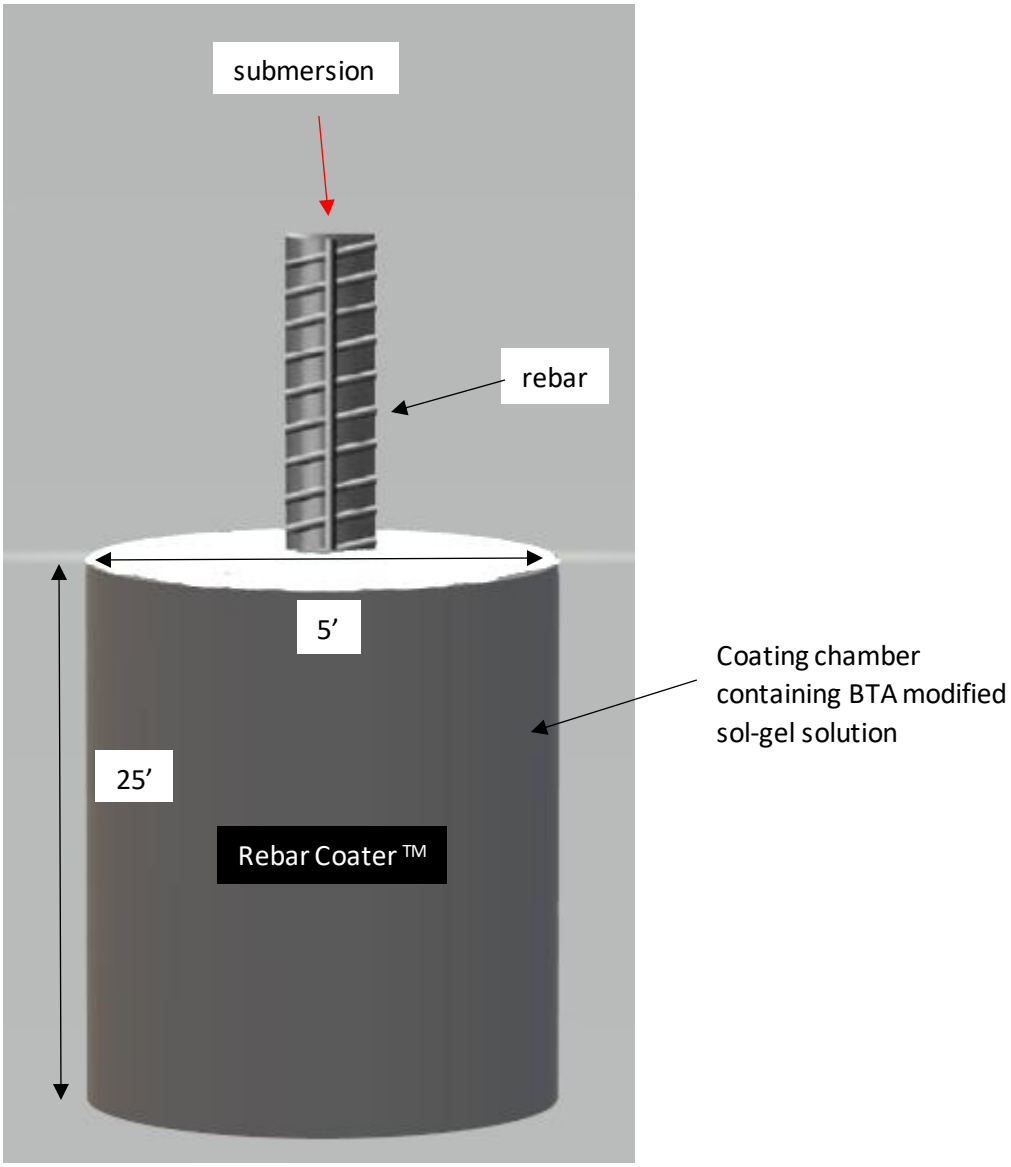

Figure 19. Dip Coating Model for Reinforced Steel

The coating chamber is 25 feet tall and 5 feet in diameter, specifically made for coating ½ inch by 20 ft rebar. Several sticks of rebar can be submerged into the *Rebar Coater* at once, which contains premade BTA modified sol-gel solution. Rebar sticks are removed after two minutes of

submersion, followed by three hours of drying at 80°C in an industrial sized oven. Post drying, the rebar's corrosion protection is immensely increased, and long-term industry use can be achieved. The *Rebar Coater* could potentially save millions of dollars each year in addition to minimizing risks of infrastructure failure (described further in Scale-up/Economics section).

Marketing

The degree to which the findings of this study could positively impact the structural integrity of reinforced concrete is extensive. As shown, BTA modified sol-gel coated carbon steel exhibited a corrosion rate significantly lower than uncoated carbon steel, suggesting that coating reinforced steel with BTA modified sol-gels will prolong lifespan of concrete infrastructures and lower risks of failure. The benefits of BTA modified sol-gels along with the designed *Rebar Coater* should be marketed toward big concrete companies such as CRH and Cemex. Prior to this marketing, however, the findings of this study must be confirmed and published by the National Association of Corrosion Engineers (NACE). If NACE confirms the immense benefits of BTA modified sol-gel coating techniques, it is very likely companies will begin surface treatment of reinforced steel using similar methods. Thus, the findings from this report should be submitted to NACE and continued research on the matter should be performed. Prior to confirmation from NACE, informal findings from this study should be directly sent to concrete companies such that these industries can begin a testing program of their own to verify the benefits of BTA modified sol-gels.

Scale-up/Economics

To discuss the ways in which the findings of this study scale up into real world application begins with a comparison of corrosion rates between blank and BTA modified sol-gel coated carbon steel.

In simulated pore solution (pH 12), blank carbon steel obtained a corrosion rate of 0.03 mm/yr compared to 0.00001 mm/yr for BTA modified sol-gel coated carbon steel. This data suggests that the corrosion performance of BTA modified sol-gel coated carbon steel is 2,680 times that of uncoated carbon steel. However, to say this would be true for reinforced steel in concrete applications would certainly be a stretch. It cannot be assumed that the lifespan and integrity of concrete infrastructure will increase by a factor of 2,680 as numerous other variables are at play, including steel stress, cement strength, etc. However, the leading cause of concrete failure in infrastructure is due to the rusting and diminished strength of reinforced steel which is the "backbone" of concrete [18]. It can be estimated that reinforced steel which undergoes surface treatment with BTA modified sol-gel films via the *Rebar Coater* will increase concrete lifespan roughly tenfold. Thus, this surface treatment technique has the potential to save billions of dollars each year in addition to providing a safer and lower risk highway bridge system in particular. While the costs of the BTA modified sol-gel films along with labor costs for steel coating application are not to be ignored, the sheer amount of money saved through the decrease of concrete repairs would make this coating technique an economical and low risk route for the long run.

Acknowledgements

The author wishes to thank Dr. Bastidas, Jacob Ress, and the University of Akron College of Engineering. The completion of this project could not be possible without the support received.

Literature Cited

[1] "A Global Need." *ECI*, corrosioninstrument.com/gn/#:~:text=The%20estimated%20cost%20to%20repair,and%20the%20cost%20of%20capital.

[2] Gelling, Victoria J, and Juan C Galván. "Enhancing the Corrosion Protection of AA2024-T3 Alloy by Surface Treatments Based on Piperazine-Modified Hybrid Sol–Gel Films." *Metals*, 21 Apr. 2020.

[3] Quraishi, MA, and DK Nayak. "Corrosion of Reinforced Steel in Concrete and Its Control: An Overview." *Journal of Steel Structures & Construction*, vol. 3, no. 1, 2017, doi: 10.4172/2472-0437.1000124.

[4] Ahmad, Zaki. "CONCRETE CORROSION." *Principles of Corrosion Engineering and Corrosion Control*, 2006.

[5] Refait, Philippe, and Anne-Marie Grolleau. "Corrosion of Carbon Steel in Marine Environments: Role of the Corrosion Product Layer." *Corrosion and Materials Degredation*, 3 June 2020.

[6] Becker, M. Chromate-free chemical conversion coatings for aluminum alloys. Corros. Rev. 2019, 37, 321–342.

[7] Rosero-Navarro, N.C.; Pellice, S.A.; Durán, A.; Aparicio, M. Effects of Ce-containing sol-gel coatings reinforced with SiO2 nanoparticles on the protection of AA2024. Corr. Sci. 2008, 50, 1283–1291.

[8] Mennucci, M M, and E P Banczek. "Evaluation of Benzotriazole as Corrosion Inhibitor for Carbon Steel in Simulated Pore Solution." *Cement and Concrete Composites*, vol. 31, no. 6, July 2009, pp. 418–424., doi:https://doi.org/10.1016/j.cemconcomp.2009.04.005.

[9] Selvi, S, and V Raman. "Evaluation of Benzotriazole as Corrosion Inhibitor for Carbon Steel in Simulated Pore Solution." *Journal of Applied Electrochemistry*, 21 July 2003.

[10] Simonović, Ana, and Žaklina Tasić. "Influence of 5-Chlorobenzotriazole on Inhibition of Copper Corrosion in Acid Rain Solution." *ACS Omega*, 29 May 2020, doi:10.1021/acsomega.0c00553.

[11] Lgaz, Hassane. "Evaluation of 2-Mercaptobenzimidazole Derivatives as Corrosion Inhibitors for Mild Steel in Hydrochloric Acid." *Metals*, 9 Mar. 2020.

[12] "1H-Benzotriazole." *National Center for Biotechnology Information. PubChem Compound Database*, U.S. National Library of Medicine, pubchem.ncbi.nlm.nih.gov/compound/1H-Benzotriazole#section=pH.

[13] Morsch, Suzanne, and Seyedgholamreza Emad. "The Unexpected Role of Carbonate Impurities in Polyphosphate Corrosion Inhibition." *Scientific Reports*, 28 Nov. 2018.

[14] L. Hamadou, A. Kadri, N. Benbrahim, Characterisation of passive films formed on low carbon steel in borate buffer solution (pH 9.2) by electrochemical impedance spectroscopy, Applied Surface Science, Volume 252, Issue 5, 2005, Pages 1510-1519

[15] Esmailzadeh, S, and M Aliofkhazraei. "Interpretation of Cyclic Potentiodynamic Polarization Test Results for Study of Corrosion Behavior of Metals." *INVESTIGATION METHODS FOR PHYSICOCHEMICAL SYSTEMS*, vol. 54, 22 June 2017, doi:10.1134/S207020511805026X.

[16] Petrunin, Maxim, and Liudmila Maksaeva. "Thin Benzotriazole Films for Inhibition of Carbon Steel Corrosion in Neutral Electrolytes." *Coatings*, 7 Apr. 2020.

[17] Faustini, Marco, and Benjamin Louis. "Preparation of Sol–Gel Films by Dip-Coating in Extreme Conditions." *The Journal of Physical Chemistry C* **2010** *114* (17), 7637-7645

[18] McCartney, Dean. "The Problem with Reinforced Concrete." *The Conversation*, 3 June 2020, theconversation.com/the-problem-with-reinforced-concrete-56078.

Appendices

Example calculation: Mass of NaCl in 150 ml of DI water for 3.5 wt% NaCl solution.

$$\text{DI water mass (g)} = 150\ \text{ml} * 1\frac{\text{g}}{\text{ml}} = 150\text{g}$$

$$\text{NaCl mass (g)} = 0.035 * 150\text{g} = 5.25\text{g}$$

Lab equipment/materials: 200 ml test cell, saturated calomel reference electrode, graphite rod counter electrode, AISI 1008 carbon steel samples, polish wheel, 300-1200 grit sandpaper, drying oven, *12A Super Spin Coater, Gamry Instruments Reference 600 Potentiostat.*

Lab chemicals: MAPTMS, TEOS, BTA, Water, Ethanol, NaCl, $Ca(OH)_2$, $NaHCO_3$, Na_2CO_3

Table 7. Molar Masses of Chemicals Used

Chemical	MAPTMS	TEOS	BTA	Water	Ethanol	NaCl	$Ca(OH)_2$	$NaHCO_3$	Na_2CO_3
Molar Mass (g/mol)	248.35	208.33	119.12	18.015	46.07	58.44	74.093	84.007	105.989

Table 8. Electrochemical Testing Matrix

	pH7	pH9	pH12
BLANK	xxx	xxx	xxx
SOL-GEL	xxx	xxx	xxx
BTA+SOL-GEL	xxx	xxx	xxx

*x is marked for a completed test

Analysis software: https://www.gamry.com/softwaredownload/GamrySoftware_7.07.6860.exe